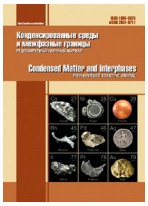

ISSN 1606-867X (Print)
ISSN 2687-0711 (Online)
Condensed Matter and Interphases
Kondensirovannye Sredy i Mezhfaznye Granitsy
https://journals.vsu.ru/kcmf/

Original articles

Research article
https://doi.org/10.17308/kcmf.2025.27/12485

Thermodynamic study of zinc antimonides by the electromotive force measurements

A. R. Aghayeva[1]✉, S. H. Mammadova[2], D. M. Babanly[1,3], Ya. I. Jafarov[4], D. B. Tagiyev[3]

[1]French-Azerbaijani University, Azerbaijan State Oil and Industry University, Nizami 183, Baku, Azerbaijan

[2]Institute of Charles Sadron of CNRS, Strasbourg 67200, France

[3]Institute of Catalysis and Inorganic Chemistry, 113 H. Javid ave., Baku, AZ-1143, Azerbaijan

[4]Baku State University, 23 Z.Khalilov, Baku Az-1048, Azerbaijan

Abstract

Zinc antimonides and phases based on them are of great interest as earth-abundant, low-cost, and environmentally friendly thermoelectric materials. The present work demonstrates the results of a thermodynamic study of the ZnSb and Zn_4Sb_3 compounds by a low-temperature electromotive force (emf) method with a glycerol electrolyte in the 300-430 K temperatures range.

Measurements were performed using equilibrium samples from the ZnSb+Sb and ZnSb+Zn_4Sb_3 two-phase regions of the Zn-Sb binary system. The phase compositions of prepared samples were controlled by means of the powder X-ray diffraction (PXRD) method. Using the least square method, the linear equations of temperature dependences of the emf data were obtained.

Based on these equations and relevant thermodynamic expressions, the partial molar Gibbs free energy, enthalpy, and entropy of zinc in alloys were calculated. Utilizing the phase diagram of the Zn-Sb system, the virtual-cell reactions for both binary compounds were determined, based on which their standard thermodynamic functions of formation and standard entropies were calculated. A comparative analysis of the obtained results with available literature data was carried out.

The results of the current work are highly accurate and can be considered a new contribution to the thermodynamics of zinc antimonides.

Keywords: ZnSb, Zn_4Sb_3, *emf* method, Electrochemical cells, Glycerol electrolyte, Thermodynamic functions

For citation: Aghayeva A. R., Mammadova S. H., Babanly D. M., Jafarov Ya. I., Tagiyev D. B. Thermodynamic study of zinc antimonides by the electromotive force measurements. *Condensed Matter and Interphases*. 2025;27(1): 48–56. https://doi.org/10.17308/kcmf.2025.27/12485

Для цитирования: Агаева А. Р., Мамедова С. Х., Бабанлы Д. М., Джафаров Я. И., Тагиев Д. Б. Термодинамическое исследование антимонидов цинка методом электродвижущих сил. *Конденсированные среды и межфазные границы*. 2025;27(1): 48–56. https://doi.org/10.17308/kcmf.2025.27/12485

✉ Aytekin R. Aghayeva, e-mail: aytekin_agayeva@mail.ru

1. Introduction

Metal pnictides are a class of compounds which are intriguing due to their promising electronic, optical, magnetic, etc. properties, that have resulted in a wide range of applications in various fields of modern technology and industry. So that binary and more complex pnictides and phases based on them are considered promising materials for applications such as high-efficiency light-emitting diodes, solar cells, quantum transport, low-power high-speed electronics, mid- to long infrared wavelength optoelectronics, thermoelectric (TE) generation and so on [1–4]. Some of them have gained recognition in physics and materials science as 3D topological Dirac semimetals and have been suggested for use as Weyl semimetals, axion insulators, and topological superconductors, making them a unique parent compound for the study of these states and the phase transitions between them [5–8].

Among binary pnictides, Zn-Sb phases are the most investigated materials showing promising TE performance. In addition, they are earth-abundant, low-cost, environmentally friendly, and stable at high temperatures up to ~1000 K materials which make them one of the best choices for the TE industry since the discovery of the Seebeck effect [9–12].

Although zinc antimonides have glass-like thermal conductivity, which makes them attractive for TE applications, their poor carrier concentration compared with state-of-the-art TE materials [13] has inspired many scientists to try to improve their electrical properties by adding dopants such as In, Al, Sn, etc. [14–16].

The phase diagram of the Zn-Sb system has been extensively studied experimentally and theoretically by many authors [17–21]. The phase diagrams reported in these studies are very similar, although the topology is slightly different. The true equilibrium phase diagram determined by a careful study considering the differences among all the previous studies was reported by H. Okamoto [22]. According to [22], Zn-Sb phase diagram is characterized by the formation of 3 antimonides: ZnSb, Zn_4Sb_3, and Zn_3Sb_2. The first compound melts at 818 K by peritectic decomposition and is stable below its melting temperature. Zn_4Sb_3 and Zn_3Sb_2 compounds have distectic melting at accordingly 837 and 838 K temperatures. Zn_4Sb_3 has 3 modifications: stable below 768 K (α-Zn_4Sb_3), between 768 and 803 K (β-Zn_4Sb_3) and above 803 K (γ-Zn_4Sb_3), respectively. Zn_3Sb_2 appears in low- and high-temperature modifications and is metastable at room temperature [22].

In a recent study, an updated phase diagram of the system Zn–Sb provides new details about the composition, transformation, and stability temperatures for the four binary phases [23]. According to the results of [23], the Zn–Sb system contains two well-known thermoelectric materials: $Zn_{1-\delta}Sb$ and $Zn_{13-\delta}Sb_{10}$ ("Zn_4Sb_3"), and two other phases: $Zn_{9-\delta}Sb_7$ and $Zn_{3-\delta}Sb_2$, which are only stable at high temperatures. The chemical formula of the well-known $Zn_{4-\delta}Sb_3$ phase was suggested as $Zn_{13-\delta}Sb_{10}$ according to its structure and composition.

Thermodynamic properties of compounds are essential for forecasting the thermal behaviour and microstructure evolution of alloys as temperature changes. As scientists explore zinc antimonides for potential applications in electronic and optoelectronic devices, a precise comprehension of their thermodynamic properties becomes imperative, paving the way for optimized performance and leveraging their capabilities in technological advancements. The thermodynamic properties of zinc antimonides were studied by different authors and summarized in modern review papers and databases [24–27]. These works are mainly dedicated to the determination of their enthalpies and Gibbs free energies of formation with calorimetric and high-temperature *emf* methods, as well as by thermodynamic assessment. Later, in the discussions section of the paper, the results of these studies will be discussed, focusing on experimental methods and models that have been used to estimate related thermodynamic properties and will be compared with the ones obtained in the current study. Therefore, to obtain a more reliable set of thermodynamic functions, it is recommended to use experimental data obtained under conditions as close as possible to the standard.

Various modifications of the *emf* method are commonly employed for the thermodynamic analysis of binary and more complex inorganic

systems. Depending on different factors such as measurement temperature, the composition of compounds, etc., different types of liquid and solid electrolytes can be applied for *emf* measurements [28-32].

Consequently, the present paper is dedicated to the thermodynamic study of zinc antimonides by low-temperature *emf* measurements.

2. Experimental part

The compositions of the prepared samples, as well as their synthesis and thermal annealing conditions were selected with respect to the phase diagram of the Zn–Sb system [22]. Alloys of different compositions from the ZnSb + Sb and ZnSb + Zn_4Sb_3 two-phase regions have been selected to study the thermodynamic properties of zinc antimonides stable at room temperature. Two samples with 52 and 70 at.% Sb composition from the ZnSb + Sb phase region and two samples with 43 and 47 at.% Sb composition from the ZnSb + Zn_4Sb_3 two-phase region of the system were selected for the thermodynamic study of the ZnSb and Zn_4Sb_3 compounds, respectively. High-purity elements (Zinc lumps - Sigma-Aldrich, CAS number 7440-66-6 and Antimony pieces - Alfa-Aesar, CAS number 7440-36-0) were used for sample preparation.

For synthesis, calculated amounts of zinc and antimony were weighed in an analytical balance and inserted into the quartz ampoules. Ampoules were evacuated up to ~ 10^{-2} Pa pressure and heated up to 900 K temperature. After 2-3 hours synthesis process, the temperature was gradually decreased to 600 K and the samples were kept at this temperature for ~500 hours.

The PXRD technique was used to confirm the phase composition of the prepared equilibrium samples. Data collection was performed at room temperature using the D2 Phaser diffractometer with Cu$K\alpha$ emission. Samples were scanned from ~ 5 to 75°. The Topas 4.2 profile modelling software was used to examine and analyse the recorder diffraction patterns.

PXRD spectrum of one sample from each phase region is given in Fig. 1. As can be seen, the PXRD spectrum of the sample with 47 at.% Sb composition (Fig. 1a) is composed of diffraction peaks of the ZnSb and Zn_4Sb_3 compounds, while the powder diffractogram of the sample with 70 at.% Sb composition (Fig. 1b) consists of diffraction lines of the ZnSb compound and an elemental antimony. Any signals belonging to other phases have not been detected in the diffraction patterns of samples, which confirms the complete synthesis and homogenization processes.

To start *emf* measurements, the following electrochemical cell was constructed:

(-) Zn(s) / glycerol + KCl + $ZnCl_2$ / Zn-Sb alloy (s) (+) (1)

The most active element of the system, namely zinc was used as the left electrode, while prepared equilibrium alloys of the Zn-Sb system were used as the right electrodes. To prepare the right electrodes, previously synthesized and annealed samples were powdered, pressed into tablets of 5-6 mm in diameter, and attached to the molybdenum rods. Molybdenum rods and electrodes were covered by glass coatings to prevent possible contact between them inside an electrolyte solution.

A liquid electrolyte of the constructed cell was a glycerol solution of KCl (Sigma Aldrich, 99.999%) with a small addition of anhydrous $ZnCl_2$ (Sigma Aldrich, 99.999%). Due to the presence of moisture and oxygen in the electrolyte, glycerol was thoroughly dehydrated and degassed at ~350 K under a dynamic vacuum. Preparation of the electrolyte and electrodes, as well as the assembly technique of the electrochemical cell (1) were put into practice as described in [33, 34].

A Keithley 2100 6 ½ The digital multimeter, having 1014 Ω input resistance and ±0.1 mV accuracy, was used to collect *emf* data in the 300- 430 K temperature interval. A chromel-alumel thermocouple and a mercury thermometer were used for temperature measurements. After keeping the cell at ~350 K for 40–60 hours, the first equilibrium values of the potential difference were obtained. Then subsequent measurements were taken every 3-4 h when a particular temperature was established. For equilibrium values of the *emf,* the difference between repeated measurements was not higher than 0.2 mV at the established temperature.

3. Results and discussions

According to experimental measurements' results, the *emf* values were constant within each

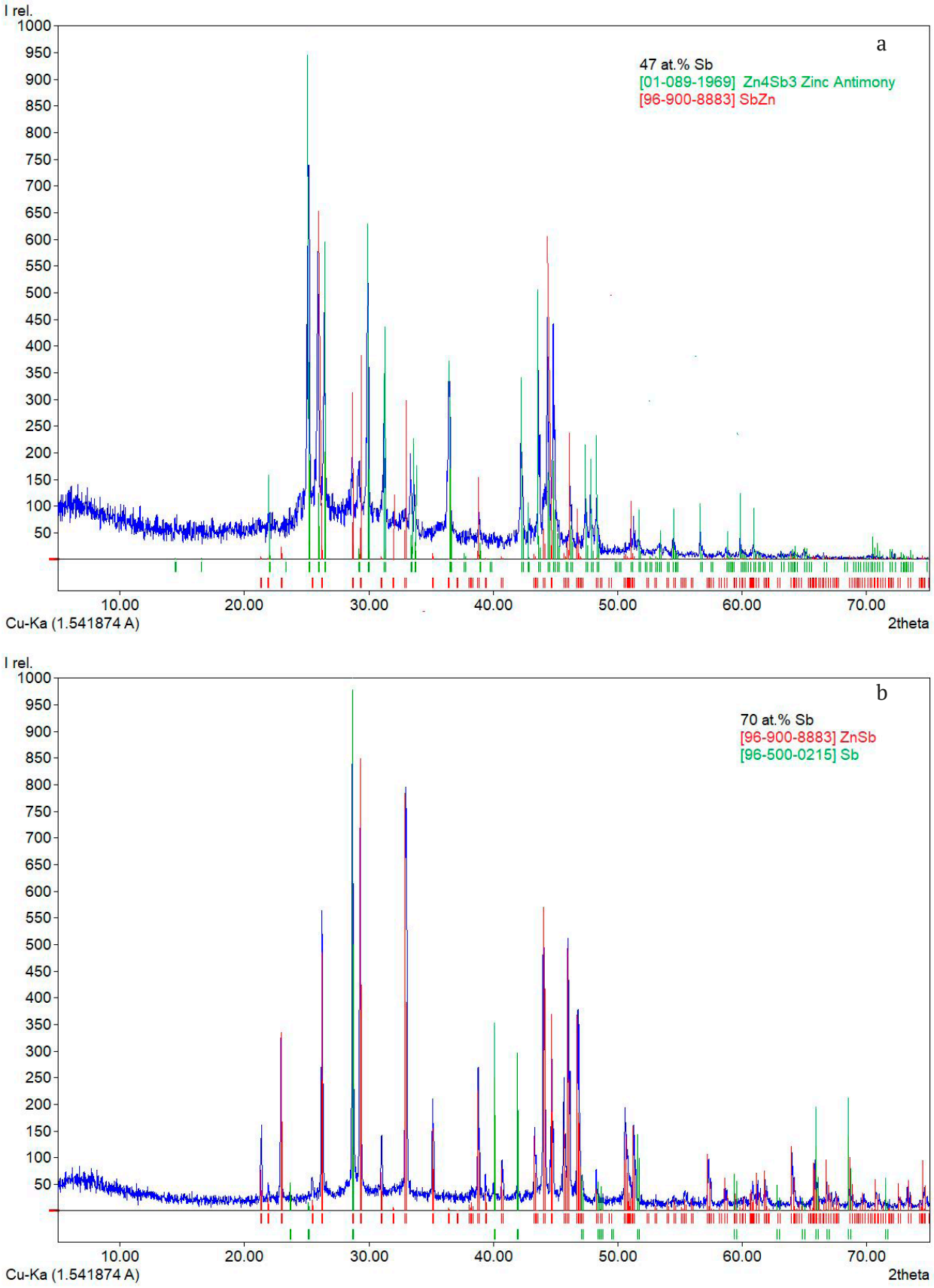

Fig. 1. PXRD spectrums of samples with a) 47 at. % Sb and b) 70 at. % Sb composition along the Zn-Sb binary system

of the ZnSb + Sb and Zn_4Sb_3+ZnSb two-phase fields, independent of the overall composition of electrode alloys. Temperature dependencies of the *emf* values for both samples are illustrated in Fig. 2. Analysis of the $E \sim f(T)$ dependences of the alloys has shown that they are practically linear (Fig. 2). It confirms the stability of the compositions of coexisting phases in above mentioned heterogeneous phase areas in the temperature range under study and gives a base for estimations of the partial entropy and enthalpy from values of the temperature coefficients of the *emf* [35, 36].

Collected experimental data were processed using least squares fitting with the Microsoft Office Excel computer program to give linear equations

$$E = a + bT \pm t\left[\frac{\delta_E^2}{n} + \delta_b^2 (T - \bar{T})^2\right]^{1/2}, \quad (2)$$

where a and b are constant coefficients, n is the number of pairs of experimental E and T values; δ_E^2 and δ_b^2 are the error variances of the *emf* readings and b coefficient, respectively; $\bar{T}$ is the average of the absolute temperature; t is Student's test. With the number of experimental points n = 30, and the confidence level equal to 95%, the student's test is $t \leqslant 2$. Obtained linear equations of the type (2) are presented in Table 1. Based on these linear equations and using the thermodynamic expressions below given, the partial molar Gibbs free energy, enthalpy, and entropy of zinc in alloys have been calculated [33–36]:

$$\Delta\bar{G}_{Zn} = -zFE, \quad (3)$$

$$\Delta\bar{S}_{Zn} = zF\left(\frac{\partial E}{\partial T}\right)_P = zFb, \quad (4)$$

$$\Delta\bar{H}_{Zn} = -zF\left[E - T\left(\frac{\partial E}{\partial T}\right)_P\right] = -zFa. \quad (5)$$

The obtained relative partial molar functions of zinc in the alloys are presented in Table 2.

According to the phase diagram of the Zn-Sb binary system [22], ZnSb compound is the richest in the antimony phase in the system and is in ZnSb + Sb equilibrium with it. Hence the partial molar functions of zinc in this region are thermodynamic functions of the following virtual-cell reaction:

$$Zn(s) + Sb(s) \rightarrow ZnSb(s). \quad (6)$$

This reaction is similar to the reaction of the formation of ZnSb compound from its elemental components. Therefore, the corresponding partial molar functions of zinc in the ZnSb + Sb phase area are standard thermodynamic functions of the formation of ZnSb.

The partial molar functions of zinc in the Zn_4Sb_3 + ZnSb two-phase field (Table 2) are thermodynamic functions of the following virtual-cell reaction:

$$Zn(s) + 3ZnSb(s) \rightarrow Zn_4Sb_3(s). \quad (7)$$

In accordance with the reaction (7), the following equations were used to calculate the standard Gibbs free energy, enthalpy, and entropy of the formation of the Zn_4Sb_3 intermediate compound:

$$\Delta_f Z^0(Zn_4Sb_3) = \Delta\bar{Z}_{Zn} + 3\Delta_f Z^0(ZnSb), \quad (8)$$

where $Z \cong G, H, or\ S$.

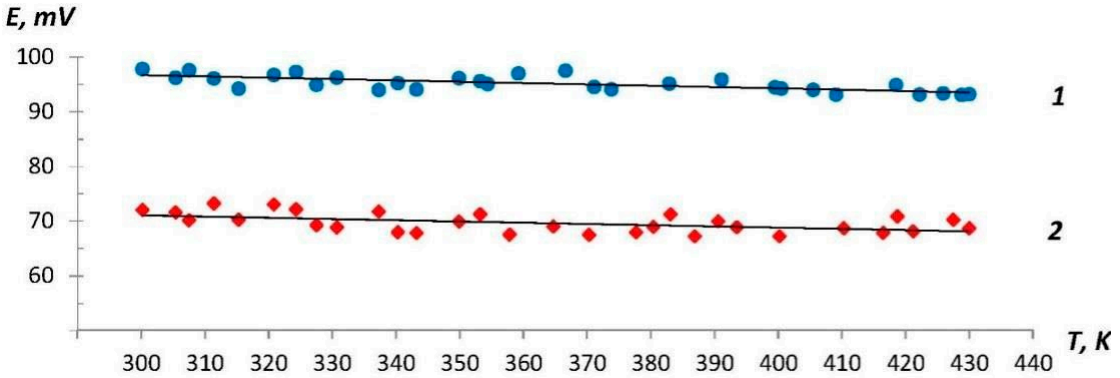

Fig. 2. $E \sim f(T)$ plots for the samples along the system Zn-Sb: (a) ZnSb +Sb phase area; (b) ZnSb + Zn_4Sb_3 phase area

Table 1. Temperature dependencies of the *emf* for the cells of the type (1) in some phase areas of the Zn–Sb system at the 300–430 K temperature interval

Phase region	$E, mV = a + bT \pm 2S_E(T)$
ZnSb(s) + Sb(s)	$103.95 - 0.0243T \pm 2\left[\frac{1.04}{30} + 2.1\cdot10^{-5}(T-363.5)^2\right]^{1/2}$
Zn_4Sb_3(s) +ZnSb(s)	$77.78 + 0.0225T \pm 2\left[\frac{2.26}{30} + 4.7\cdot10^{-5}(T-363.2)^2\right]^{1/2}$

Table 2. Partial molar thermodynamic functions of zinc in the alloys of the Zn–Sb system at 298 K

Phase region	$-\Delta\bar{G}_{Zn}$, kJ/mol	$\Delta\bar{H}_{Zn}$, kJ/mol	$\Delta\bar{S}_{Zn}$, J/(mol·K)
ZnSb(s) + Sb(s)	18.66±0.14	20.06±0.64	–4.69±1.76
Zn_4Sb_3(s) + ZnSb(s)	13.71±0.20	15.01±0.98	–4.36±2.66

Absolute entropies of the ZnSb and Zn_4Sb_3 compounds have been calculated using the following equations:

$$S^0(\mathrm{ZnSb}) = \Delta\bar{S}_{Zn} + S^0_{Zn} + S^0_{Sb} \quad (9)$$

$$S^0(\mathrm{Zn_4Sb_3}) = \overline{\Delta S}_{Zn} + S^0{}_{Zn} + 3S^0{}_{ZnSb}. \quad (10)$$

Errors were calculated by the error accumulation method. Absolute entropies of the elementary zinc and antimony used for calculations were taken from [25]: $S°$(Zn) = 41.63±0.13 J/(mole·K); $S°$(Sb) = 45.69±0.63 J/(mole·K). Calculated standard integral thermodynamic functions of both compounds along with available literature data are tabulated in Table 3.

The $\Delta_f G°$ values in the table related to the studies with the *emf* measurements [38-40, 46] were calculated by us for 298 K based on the results of those studies. Comparative analysis of the values in the table shows that the results of the current study for the ZnSb compound are in good agreement with the results of the *emf* measurements given in [37, 38], obtained by vapor pressure measurement method [41], as well as

Table 3. Standard integral thermodynamic functions of zinc antimonides

Compound	$-\Delta_f G°$	$-\Delta_f H°$ kJ/mol	$\Delta_f S°$ J/(mol·K)	$S°$	Reference, method
ZnSb	18.7±0.2	20.1±0.7	–4.7±1.8	82.6±2.5	This work, *emf*
	19.89	21.80			[37], *emf*
	17.75	19.10			[38], *emf*
	16.28	16.46			[39], *emf*
	16.53	17.15			[40], *emf*
	17.68	19.00			[41], vap. press.
		12.8			[42], calorimetry
		74.47			[43], calorimetry
	19.5	22.49			[17], optimization
	20.36	22.98			[44], optimization
		22.92			[45], optimization
		19.0±1.3		82.6±1.7	[24], recommend
	17.40	16.74		89.54±2.1	[25], recommend
	17.72	18.93		83.08	[26], recommend
Zn_4Sb_3	69.7±0.7	75.2±3.0	–18.5±7.9	285.1±10.4	This work, *emf*
	65.30	74.90			[37], *emf*
	55.48	37.24			[39], *emf*
	56.82	54.79			[46], *emf*
	61.31	65.57			[44], optimization
	65.02	65.65			[47], optimization

with the ones thermodynamically optimized in [17, 44, 45]. The results obtained from other *emf* studies are somewhat lower. Quantities obtained during two different calorimetric studies differ from each other by more than 5 times, and hence they are naturally insignificant. It should also be noted that for the ZnSb compound, the quantities provided in the reference books [24-26] are slightly different than our results. Among them, the results of [24] and [26] are in better agreement with the current study.

Thermodynamic properties of the Zn_4Sb_3 compound were experimentally studied only using the *emf* method [37, 39, 46] until our studies and their thermodynamic optimization were carried out by [44, 47]. As can be seen from Table 3, our results are closer to [37] and also agree with the optimized thermodynamic quantities.

Thus, the obtained standard thermodynamic functions have high accuracy and minimize existing contradictions, especially for the standard entropy and Gibbs free energy of formation for both compounds.

4. Conclusion

The present contribution shares the results of the thermodynamic study of the ZnSb and Zn_4Sb_3 compounds by a low-temperature *emf* method. Using samples from the ZnSb+Sb and Zn_4Sb_3+ZnSb phase areas of the system as a right electrode, the linear equations of temperature dependences of the *emf* have been obtained. From these linear equations, the partial molar thermodynamic functions of zinc in alloys have been calculated. Based on the *T-x* diagram of the Zn-Sb system, the potential generating reactions for both binary compounds have been defined and consequently, their standard integral thermodynamic functions have been determined. The set of obtained standard thermodynamic quantities is of high accuracy and a new contribution to the thermodynamics of zinc stibnites. These results allow us to minimize the contradictions between the existing literature data.

Contribution of the authors

The authors contributed equally to this article.

Conflict of interests

The authors declare that they have no known competing financial interests or personal relationships that could have influenced the work reported in this paper.

References

1. Assoud A., Kleinke H. *Metal pnictides: structures and thermoelectric properties*. *Handbook of Solid-State Chemistry*. 2017. https://doi.org/10.1002/9783527691036.hsscvol1012

2. Rasaki S. A., Thomas T., Yang M. Iron based chalcogenide and pnictide superconductors: from discovery to chemical ways forward. *Progress in Solid State Chemistry*. 2020;59: 100282. https://doi.org/10.1016/j.progsolidstchem.2020.100282

3. Kumar J., Gautam G. S. Study of pnictides for photovoltaic applications. *Physical Chemistry Chemical Physics*. 2023;25(13): 9626–9635. https://doi.org/10.1039/D2CP04453F

4. Marchand R., Jeitschko W. Ternary lanthanoid-transition metal pnictides with $ThCr_2Si_2$-type structure. *Journal of Solid-State Chemistry*. 1978;24(3-4): 351–357. https://doi.org/10.1016/0022-4596(78)90026-9

5. Liu Z. K., Jiang J., Zhou B., …Chen Y. L. A stable three-dimensional topological Dirac semimetal Cd_3As_2. *Nature Materials*. 2014;13(7): 677–681. https://doi.org/10.1038/nmat3990

6. Liu Z. K., Zhou B., Zhang Y., … Chen Y. L. Discovery of a three-dimensional topological Dirac semimetal, Na_3Bi. *Science*. 2014;343(6173): 864–867. https://doi.org/10.1126/science.1245085

7. Wang Z., Weng H., Wu Q., Dai X., Fang Z. Three-dimensional Dirac semimetal and quantum transport in Cd_3As_2. *Physical Review B – Condensed Matter and Materials Physics*. 2013;88(12): 125427. https://doi.org/10.1103/PhysRevB.88.125427

8. Crassee I., Sankar R., Lee W. L., Akrap A., Orlita M. 3D Dirac semimetal Cd_3As_2: a review of material properties. *Physical Review Materials*. 2018;2(12): 120302. https://doi.org/10.1103/PhysRevMaterials.2.120302

9. Song X., Finstad T. G. Review of research on the thermoelectric material ZnSb. *Thermoelectrics for power generation: a look at trends in the technology*. 2016. https://doi.org/10.5772/65661

10. Castellero A., Fanciulli C., Carlini R., … Baricco M. Effect of processing routes on the synthesis and properties of Zn_4Sb_3 thermoelectric alloy. *Journal of Alloys and Compounds*. 2015;653: 54–60. https://doi.org/10.1016/j.jallcom.2015.08.251

11. Sreeparvathy P. C., Kanchana V., Vaitheeswaran G. Thermoelectric properties of zinc based pnictide semiconductors. *Journal of Applied Physics*. 2016;119(8): 085701. https://doi.org/10.1063/1.4942011

12. Bjerg L., Madsen G. K. H., Iversen B. B. Enhanced thermoelectric properties in zinc antimonides. *Chemistry of Materials*. 2011;23(17): 3907–3914. https://doi.org/10.1021/cm201271d

13. Snyder G. J., Toberer E. S. Complex thermoelectric materials. *Nature Materials*. 2008;7(2): 105–114. https://doi.org/10.1038/nmat2090

14. Ostovari Moghaddam A., Shokuhfar A., Zhang Y., … Cabot A. Ge-doped ZnSb/β-Zn_4Sb_3 nanocomposites with high thermoelectric performance. *Advanced Materials Interfaces*. 2019;6(18): 1900467. https://doi.org/10.1002/admi.201900467

15. Carlini R., Marré D., Pallecchi I., Ricciardi R., Zanicchi G. Thermoelectric properties of Zn_4Sb_3 intermetallic compound doped with aluminum and silver. *Intermetallics*. 2014;45: 60–64. https://doi.org/10.1016/j.intermet.2013.10.002

16. Gau H. J., Yu J. L., Wu C. C., Kuo Y. K., Ho C. H. Thermoelectric properties of Zn–Sb alloys doped with In. *Journal of Alloys and Compounds*. 2009;480(1): 73–75. https://doi.org/10.1016/j.jallcom.2008.09.202

17. Liu X. J., Wang C. P., Ohnuma I., Kainuma R., Ishida K. Thermodynamic assessment of the phase diagrams of the Cu-Sb and Sb-Zn systems. *Journal of Phase Equilibria*. 2000;21: 432–442. https://doi.org/10.1361/105497100770339608

18. Izard V., Record M. C., Tedenac J. C., Fries S. G. Discussion on the stability of the antimony zinc binary phases. *Calphad*. 2001;25(4): 567–581. https://doi.org/10.1016/S0364-5916(02)00008-1

19. Adjadj F., Belbacha E. D., Bouharkat M., Kerboub A. Crystallographic study of the intermediate compounds SbZn, Sb_3Zn_4 and Sb_2Zn_3. *Journal of Alloys and Compounds*. 2006;419(1-2): 267–270. https://doi.org/10.1016/j.jallcom.2005.09.068

20. Adjadj F., Belbacha E. D., Bouharkat M. Differential calorimetric analysis of the binary system Sb–Zn. *Journal of alloys and compounds*. 2007;430(1-2): 85–91. https://doi.org/10.1016/j.jallcom.2006.04.051

21. Li J. B., Record M. C., Tedenac J. C. A thermodynamic assessment of the Sb–Zn system. *Journal of Alloys and Compounds*. 2007;438(1-2): 171–177. https://doi.org/10.1016/j.jallcom.2006.08.035

22. Okamoto H. Sb-Zn (Antimony-Zinc). *Journal of Phase Equilibria and Diffusion*. 2008;29: 290–290. https://doi.org/10.1007/s11669-008-9315-y

23. Lo C. W. T., Svitlyk V., Chernyshov D., Mozharivskyj Y. The updated Zn–Sb phase diagram. How to make pure $Zn_{13}Sb_{10}$ ("Zn_4Sb_3"). *Dalton Transactions*. 2018;47(33): 11512–11520. https://doi.org/10.1039/C8DT02521E

24. Kubaschewski O., Alcock C. B., Spenser P. *Materials Thermochemistry*. Oxford: Pergamon Press; 1993. 6th edn. 363 p.

25. Iorish V. S., Yungman V. S. (eds.). *Thermal constants of substances: database, 2006. Version 2.*

26. Barin I. *Thermochemical data of pure substances*. New York: Wiley-VCH; 2008. 3rd edn. 2003 p.

27. Schlesinger M. E. Thermodynamic properties of solid binary antimonides. *Chemical Reviews.* 2013;113(10): 8066–8092. https://doi.org/10.1021/cr400050e

28. Aliev Z. S., Babanly M. B., Shevelkov A. V., Babanly D. M., Tedenac J. C. Phase diagram of the Sb–Te–I system and thermodynamic properties of SbTeI. *International journal of materials research*. 2012;103(3): 290–295. https://doi.org/10.3139/146.110646

29. Imamaliyeva S. Z., Musayeva S. S., Babanly D. M., Jafarov Y. I., Taghiyev D. B., Babanly M. B. Determination of the thermodynamic functions of bismuth chalcoiodides by EMF method with morpholinium formate as electrolyte. *Thermochimica Acta*. 2019;679: 178319. https://doi.org/10.1016/j.tca.2019.178319

30. Aliev Z. S., Musayeva S. S., Imamaliyeva S. Z., Babanly M. B. Thermodynamic study of antimony chalcoiodides by EMF method with an ionic liquid. *Journal of Thermal Analysis and Calorimetry*. 2018;133: 1115–1120. https://doi.org/10.1007/s10973-017-6812-4

31. Alverdiyev I. J., Aliev Z. S., Bagheri S. M., Mashadiyeva L. F., Yusibov Y. A., Babanly M. B. Study of the $2Cu_2S + GeSe_2 \leftrightarrow 2Cu_2Se + GeS_2$ reciprocal system and thermodynamic properties of the $Cu_8GeS_{6-x}Se_x$ solid solutions. *Journal of Alloys and Compounds*. 2017;691: 255–262. https://doi.org/10.1016/j.jallcom.2016.08.251

32. Mashadiyeva L. F., Mammadli P. R., Babanly D. M., Ashirov G. M., Shevelkov A. V., Yusibov Y. A. Solid-phase equilibria in the Cu-Sb-S system and thermodynamic properties of copper-antimony sulfides. *JOM*. 2021;73: 1522–1530. https://doi.org/10.1007/s11837-021-04624-y

33. Babanly M. B., Yusibov Y. A. *Electrochemical methods in thermodynamics of inorganic systems*. Baku: BSU Publ.; 2011. 306 p.

34. Morachevsky A. G., Voronin G. F., Heiderich V. A., Kutsenok I. B. *Electrochemical methods of research in the thermodynamics of metallic systems*. ICC "Akademkniga" Publ.; 2003. 334 p.

35. Babanly M. B., Yusibov Y. A., Babanly N. B. In: *Electromotive force and measurement in several systems.* S. Kara (ed.). London: Intechweb. Org; 2011. p. 57. https://doi.org/10.5772/28934

36. Shao Y. (ed.). *Electrochemical cells – new advances in fundamental research and applications*. London: InTech; 2012. 252 p. https://doi.org/10.5772/1890

37. Goryacheva V. I., Geiderikh V. A. The thermodynamic properties of phases in the zinc-antimony system. *Russian Journal of Physical Chemistry A*. 1997;71(4): 526–529.

38. Goncharuk L. V, Lukashenko G. M. Thermodynamic properties of zinc antimonides. *Journal of Applied Chemistry. USSR (Engl. Transl.)*. 1988;62(8): 10.

39. Zabdyr L. A. Thermodynamic properties of zinc antimonides. *Canadian Metallurgical Quarterly*. 1980;19(4): 359–362. https://doi.org/10.1179/cmq.1980.19.4.359

40. Eremenko V. N., Lukashenko G. M. Thermodynamic properties of higher zinc antimonide. *Russian Journal of Inorganic Chemistry. (Engl. Transl.)*. 1963;8(3).

41. Hirayama C. The dissociation pressure of zinc antimonide. *Journal of The Electrochemical Society*. 1963;110(1): 88. https://doi.org/10.1149/1.2425680

42. Stolyarova T. A. Enthalpy of formation of zinc antimonite ZnSb. *Russian Metallurgy (Metally). (Engl. Transl.)*. 1979;6: 61.

43. Shchukarev S. A., Morozova M. P., Sapozhnikov Yu. P. Enthalpy of formation of compounds of zinc with antimony. *Journal of General Chemistry of the USSR (Engl. Transl.)*. 1956;26: 321.

44. Liu Y., Tedenac J. C. Thermodynamic modeling of the Cd–Sb–Zn ternary system. *Calphad*. 2009;33(4): 684–694. https://doi.org/10.1016/j.calphad.2009.08.006

45. Li J. B., Record M. C., Tedenac J. C. A thermodynamic assessment of the Sb–Zn system. *Journal of Alloys and Compounds*. 2007;438(1-2): 171–177. https://doi.org/10.1016/j.jallcom.2006.08.035

46. Seltz H., DeWitt B. J. A thermodynamic study of the lead-antimony system. *Journal of the American Chemical Society*. 1939;61(10): 2594–2597. https://doi.org/10.1021/ja01265a007

47. Zabdyr L. A. Equilibrium diagram and thermodynamic properties of cadmium—antimony binary alloys. Critical assessment. *Calphad*. 1993;17(2): 125–132. https://doi.org/10.1016/0364-5916(93)90012-Z

Information about the authors

Aytekin R. Aghayeva, PhD student in physical chemistry, Laboratory assistant, Physics Department, French-Azerbaijani University, (Baku, Azerbaijan).
https://orcid.org/0000-0001-8184-0762
aytekin_agayeva@mail.ru

Sakina H. Mammadova, PhD student in polymer chemistry, Institute of Charles Sadron of CNRS (Strasbourg, France).
https://orcid.org/0009-0000-5731-9993
sakina.mammadova@ufaz.az

Dunya M. Babanly, Dr. Sci. (Chem.), Assoc. Professor, Head of the Chemistry Department, researcher-teacher, French-Azerbaijani University (Baku, Azerbaijan).
https://orcid.org/0000-0002-8330-7854
dunya.babanly@ufaz.az

Yasin I. Jafarov, Dr. Sci. (Chem.), Professor, Head of the General and Inorganic Chemistry Department, Baku State University (Baku, Azerbaijan).
https://orcid.org/0000-0002-3968-8725
yasin.cafarov@hotmail.com

Dilgam B. Tagiyev, Professor (Chem.), Academician, Vice-President of the National Academy of Sciences of Azerbaijan, General Director of the "Institute of Catalysis and Inorganic Chemistry" (Baku, Azerbaijan).
https://orcid.org/0000-0002-8312-2980
dtagiyev@rambler.ru

Translation by the author